

Offspring of SPACE: the Spectrograph Channel of the ESA Dark Energy Mission EUCLID

Robert Content^{*a}, Andrea Cimatti^b, Massimo Robberto^c, Robert Grange^d, Paolo Spano^e, Ray M. Sharples^a, Carlton M. Baugh^f, Bianca Garilliⁱ, Luigi Guzzo^e, Olivier Le Fevre^d, Dario Maccagniⁱ, Piero Rosati^j, Yun Wang^g, Giovanni Zamorani^h, Filippo Zerbi^e

^aCentre for Advanced Instrumentation, dept. of Physics, U. of Durham, South Road, Durham City, U.K. DH1 3LE;

^bDipartimento di Astronomia, Alma Mater Studiorum - Università di Bologna, Via Ranzani 1, I-40127, Italy;

^cSpace Telescope Science Institute, 3700 San Martin Dr., Baltimore, MD USA 21218;

^dLaboratoire d'Astrophysique de Marseille, CNRS and U. de Provence, Pole de l'Etoile Site de Chateau-Gombert, 38 rue Frédéric Joliot-Curie, 13388 Marseille cedex 13 France;

^eINAF - Osservatorio Astronomico di Brera, Via Emilio Bianchi 46 - I-23807 Merate - ITALY;

^fInstitute for Computational Cosmology, dept. of Physics, U. of Durham, South Road, Durham City, U.K. DH1 3LE;

^gDept. of Physics & Astronomy, U. of Oklahoma, Norman, OK USA 73019;

^hINAF - Bologna Astronomical Observatory, Via Ranzani 1, 40127 Bologna, Italy;

ⁱINAF, IASF-Milano, via Bassini 15, 20133 Milano, Italy;

^jESO-European Southern Observatory, Karl-Schwarzschild-Strasse 2, D-85748, Garching bei München, Germany.

ABSTRACT

The SPACE and DUNE proposals for the ESA Cosmic Vision 2015-2025 have been pre-selected for a Dark Energy Mission. An assessment study was performed in the past few months resulting in a merged mission called EUCLID. The study led to a possible concept for the mission and the payload, paving the way for the industrial studies. SPACE has now become the EUCLID spectrograph channel (EUCLID-spectro). We will discuss its science and give a description of the different studied optical designs. EUCLID-spectro aims to produce the largest three-dimensional map of the Universe by taking near-IR spectra at $R=400$ and $0.9\mu\text{m} < \lambda < 1.7\mu\text{m}$ for ~ 200 million galaxies at $z < 2$ and $H < 22$ over $20,000 \text{ deg}^2$. It will measure the expansion history of the Universe and the growth rate of structure using Baryonic Acoustic Oscillations, redshift-space distortions and clusters of galaxies. It will distinguish true dark energy from a modification of Einstein's gravity. The original design had 4 channels each re-imaging with mirrors a sub-field from the Casgrain focus onto a Digital Micromirror Device (DMD). A prism spectrograph followed each array. This design was modified to adapt EUCLID-spectro to a DUNE-type telescope, to reduce the number of optics and spectrographs, and add an imaging capability. We studied grism spectrographs, especially for a slitless backup solution that have less optics but a smaller field; we also studied compact prism and lens spectrographs, telescope corrector combined with micromirror arrays at the Casgrain focus then eliminating the re-imaging, and TIR prisms over the arrays to help with packaging.

Keywords: dark energy, space telescope, multi-object spectroscopy.

1. INTRODUCTION

Our view of the Universe has changed dramatically over the past two decades through measurements of the cosmic microwave background (CMB), the large-scale structure of the local Universe ($z < 0.3$) and the brightness of distant supernovae. Fully 96% of the constituents consist of non-luminous and unidentified dark energy (73%) and dark matter

*robert.content@durham.ac.uk; phone: +44-191-334-3541

(23%) that govern the expansion history and evolution of cosmic structure and leave their imprints on the structure and distribution of visible galaxies. These dark components are unexplained in standard physical theory, but are, nevertheless, considered a natural feature of standard cosmology because they can explain a wide range of observations assuming only that dark energy produces a pressure countering gravity and dark matter behaves like ordinary matter in its effect on space-time.

The SPACE and DUNE proposals primarily aimed at getting a much better understanding of dark energy by making measurements on far away galaxies. While SPACE uses multi-object spectroscopy to measure redshift, DUNE uses imaging to measure weak lensing. Both were proposed missions for the ESA Cosmic Vision 2015-2025. However, ESA did not choose one mission or the other or both but pre-selected both proposals for one dark energy mission. A pre-phase A study was then necessary to clarify this situation. The 3 choices were a) keep SPACE and drop DUNE, b) keep DUNE and drop SPACE, and c) merge the 2 missions. The latter was the preferred solution of ESA which see in this option a minimum multiplex advantage of 2, possibly 4, compared to the option of keeping one of the 2 missions. The assessment study was performed in the past few months resulting in a merged mission called EUCLID. The study led to a possible concept for the mission and the payload ^[4], paving the way for the industrial studies. The SPACE payload became the EUCLID spectrograph channel. The present paper describes the scientific background of the instrument and the different designs and design options that were studied for the assessment study.

Table 1. EUCLID-spectro main characteristics.

Spectral resolution (average)	400
Baseline wavelength range	0.9 to 1.7 μm
Field of view	0.82° x 0.57°
Sky coverage	20,000 deg ²
Total number of galaxies	200,000,000
Detector size	2048 x 2048
Number of detectors per spectrograph	2
Number of spectrographs	3
Telescope primary diameter	1.2-m
Digital Micromirror Device size	2048 x 1080



Fig. 1. Typical substructure of a TI DMD (left); DMD array with an ant leg for comparison (centre); DMD CINEMA (right).

2. DMD

In the different designs of the EUCLID spectrograph channel, images of different parts of the sky are obtained on a few Digital Micromirror Devices (DMDs). Each contains an array of addressable micromirrors that can be placed in one of 2 positions. In the "ON" position, the beam from the micromirror enters the spectrograph. In the "OFF" position, the beam is sent to a light dump. Fig. 1 shows the structure of a DMD and how small the micromirrors are, here 13.7 μm . The

DMD CINEMA has been used as the reference in all our designs. It has 2048 x 1080 micromirrors that can be tilted by +/- 12°. The beam is then displaced by 48° when the micromirror moves between ON and OFF positions.

3. SCIENTIFIC BACKGROUND

The acceleration of the expansion of the Universe is considered one of the most important discoveries of cosmology^[1,2]. Both of the extant explanations for accelerating space-time require new physics: a negative pressure component dubbed dark energy, or a modification of the law of gravity and, therefore, the standard framework underpinning cosmology. The first possibility, dark energy, is currently favored but, nevertheless, provides little help because we have no plausible candidates from elementary particle theories. The simplest case is represented by the so-called cosmological constant, Λ . Unfortunately, there is no theoretical justification for the size of the cosmological constant as inferred from the rate of universal acceleration. Arguments based on the standard model of particle physics yield values between 10^{50} and 10^{123} times larger than the observed value. The cosmological constant is only one of several candidates to explain the acceleration of the universe. Most possibilities can be parameterized by their equation of state, the ratio of the pressure exerted by the dark energy to the energy density of the field: $w = P/\rho c^2$. A cosmological constant necessarily implies $w = -1$. The simplest alternative quantum-field explanations allow w to differ from -1 and to vary with time. Translating from linear time to observable redshift, z , we can parameterize $w(z) = w_0 + w_a(1-a)$, $a=1/(1+z)$. The magnitude of w determines the rate of acceleration (through the associated pressure), so it can be characterized by measuring the rate of acceleration as a function of time for the history of the Universe, or equivalently, the Hubble parameter as a function of redshift, $H(z)$. Alternatively, the acceleration could be the result of a modified form of gravity, such as gravity that is a function of scale, or a modification of the standard model through string or brane theories. Distinguishing between dark energy, modified gravity and different variants necessarily requires high-precision measurements of the cosmic expansion rate history $H(z)$, but the remaining differences among theories mean that even a very accurate $H(z)$ is inadequate to uniquely isolate one theory. The degeneracy occurs because a dark energy model and a modified gravity theory can give identical cosmic expansion histories $H(z)$, but would give very different growth histories of cosmic large scale structure. Since the predicted growth rate of large-scale structures varies among theories, a measurement of structure evolution can isolate the correct one. The best current constraints on w from observations of distant supernovae are consistent with a cosmological constant: $-1 < w < -0.85$ with 10%-20% uncertainties assuming a flat Universe.

The cosmological models make testable predictions about how the dark components affect a wide range of observable features that can be discriminated with high precision only using newly developed technology on spacecraft. This is the framework in which we have proposed a new space mission aimed at addressing the key questions of modern cosmology in response to the ESA call *Cosmic Vision 2015-2025*. Our proposal for a *SP*ectroscopic *All-sky Cosmic Explorer* (*SPACE*) has subsequently been merged with a weak-lensing imaging mission (*DUNE*), to become *Euclid*, the European Dark Energy Mission. To solve the mystery of dark energy, the spectroscopic channel on *Euclid* will determine $H(z)$ and constrain w_0 and w_a by combining the observations of the Baryonic Acoustic Oscillations (BAO), the growth rate of structures, distant Type Ia Supernovae and high redshift galaxy clusters. Combining the spectroscopic and imaging approaches to dark energy will increase the accuracy of the determination of w by a factor ~ 2 , and reduce the sensitivity to different systematics. The mission will also address several other key questions of modern cosmology besides dark energy. Further details on the main scientific objectives of *SPACE* can be found in^[3].

4. DMD AT DIRECT TELESCOPE FOCUS

To reduce the space envelope for a spectroscopic arm, DMD chips can be put directly in front of the telescope focal plane. The fastest possible focal ratio for the DMD is about F/2.5, maximizing FoV for each spectrograph. At the same time, such a fast beam cannot be achieved with a two-mirror telescope without a very large secondary mirror, reducing collecting area.

A fast F/4, 1.2-m diameter, two-mirror Ritchey-Chrétien telescope, with a double corrector plate, has been designed giving a corrected field of view of 1.5 deg (fig. 2) and a plate scale of 23 $\mu\text{m}/\text{arcsec}$. This large FoV can feed both an imaging (on-axis) channel and one or more spectroscopic channels, through lateral pick-up mirrors that each sends the beam towards a DMD. The telescope has negligible distortion, but a curved image plane (R 787mm). This will translate

into a defocus of 16 micron. Image quality is near-diffraction limited over the full field of view for the selected wavelength range (Fig. 3).

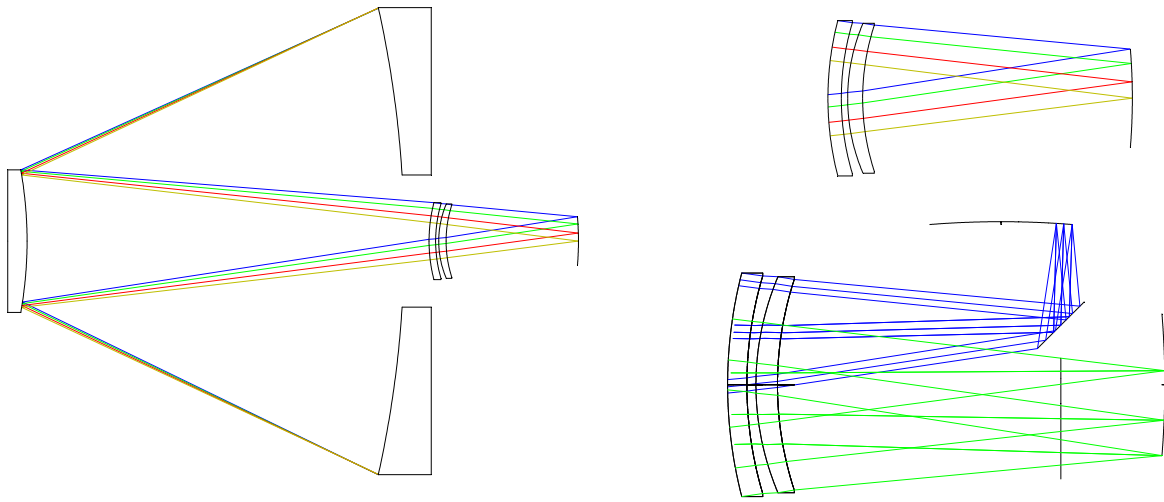


Fig. 2. Optical layout of the telescope (left), with enlarged views of the double-corrector plate and a pick-up mirror (right).

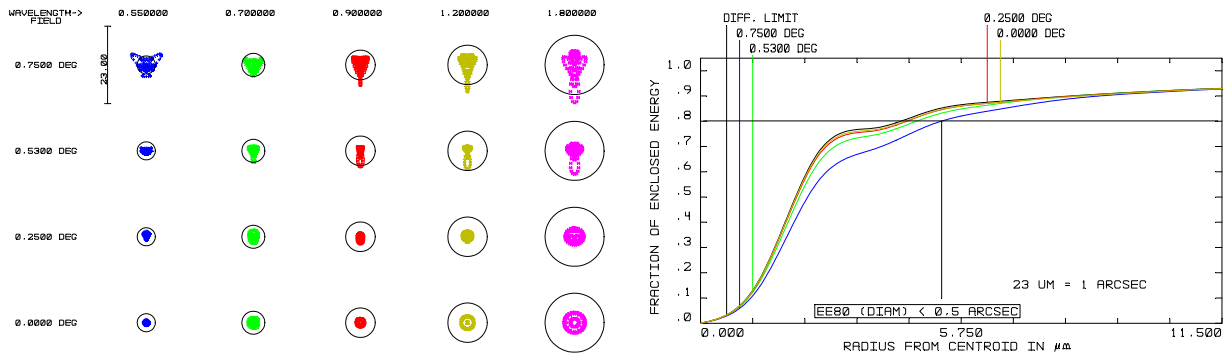


Fig. 3. Left: spot diagrams for the telescope at different wavelengths and field of view. Circles represent Airy disks. Right: MTF curves show that 80% encircled energy follows within 0.5 arcsec.

5. TIR SPECTROGRAPHS

To reduce the overall space envelope, total internal reflection (TIR) prisms can be used in front of the DMD chips. They allow separating incoming and outgoing beams without any need of large optical components before and after the DMD. Glasses and prism angles must be selected to give high optical quality for the projected image onto the DMD chip, high efficiency, and high rejection of unwanted light to increase the contrast.

Among different kinds of TIR prism layouts, we selected one with smaller aberrations (Fig. 4). These aberrations (mainly coma, astigmatism, and chromaticity) can be minimized by reducing both the thickness of the prism and the incidence angles on its surfaces. To allow a “straight” path between the incoming and outgoing beams, a flat folding mirror between the corrector and the TIR prism can be placed.

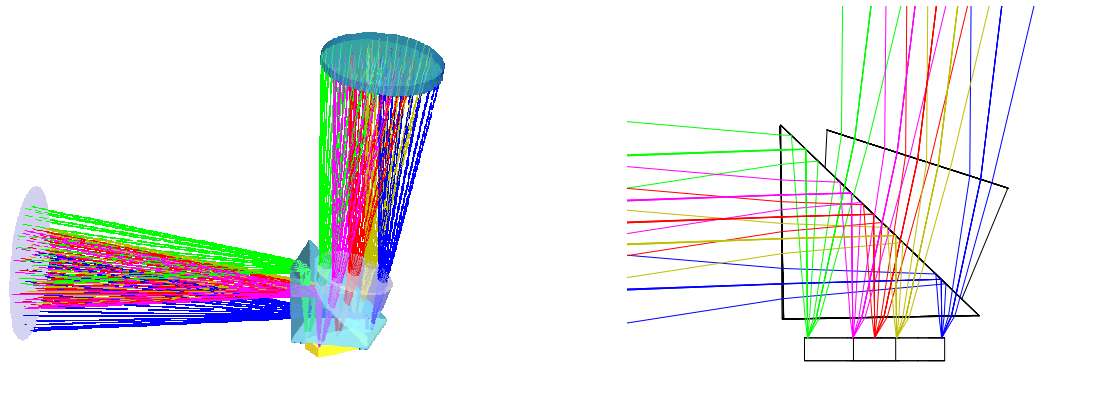


Fig. 4. Optical layout of a total internal reflection prism (TIR) used to image the focal plane at the right angle. After target selection on the DMD surface, lights is sent back at normal incidence and is reflected by the prism.

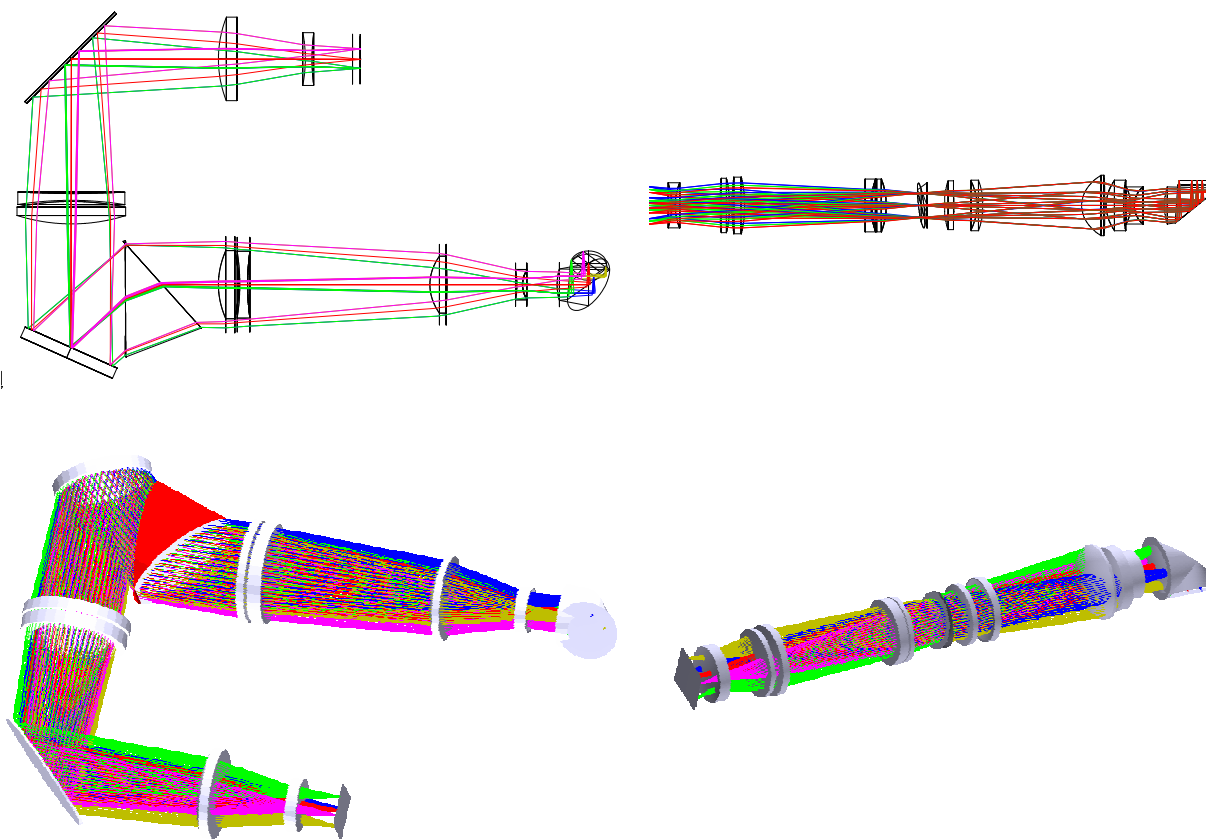


Fig. 5. Optical layout of a prism spectrograph (left) and a grism spectrograph (right) using TIR prism to inject light. These two layouts are not to scale.

Once a proper TIR prism has been designed, the spectrograph design can be easily built with only lenses, both for collimator and camera optics. Two different solutions are proposed, where different dispersers are used: with a flint prism or a grism. The latter one is the smallest, due to the higher angular dispersion of the grism.

5.1 TIR spectrograph with prism disperser

In this solution, light from the DMD chip is folded at 90° inside the TIR prism and is directed towards an F/4 collimator made of four lenses, creating a pupil of 70 mm diameter onto the disperser, a prism. After being dispersed, light hit a folding mirror and is sent to the camera optics. To have a more compact layout, another folding mirror has been added inside the camera. Overall dimension is 55 x 35 cm. The prism is quite small and light. Figure 5 (left) shows a possible layout for such a spectrograph.

5.2 TIR spectrograph with grism disperser

If a grism is used instead of a prism as cross-disperser, a very compact layout can be designed, taking full advantage of the larger dispersion of a grism. Of course, it will reduce the overall spectral coverage, with a smaller efficiency, due to grism typical characteristics, and many parasite orders. Figure 5 (right) shows a possible straight layout, being enclosed within a cylinder of 7cm x 47 cm.

Optical components have been designed for a 35mm collimated beam, with a very high image quality. The number of elements can then be decreased and still gives acceptable performances after re-optimization. Due to the grism, the spectral coverage (to suppress unwanted orders) will be limited from 0.9 to 1.75 μm . No tilts of optical components are required, excluding the grism and the detector that are rotated along the optical axis, to cope with the behavior of the DMD pixels. If folding mirrors will be added, other solutions can be designed.

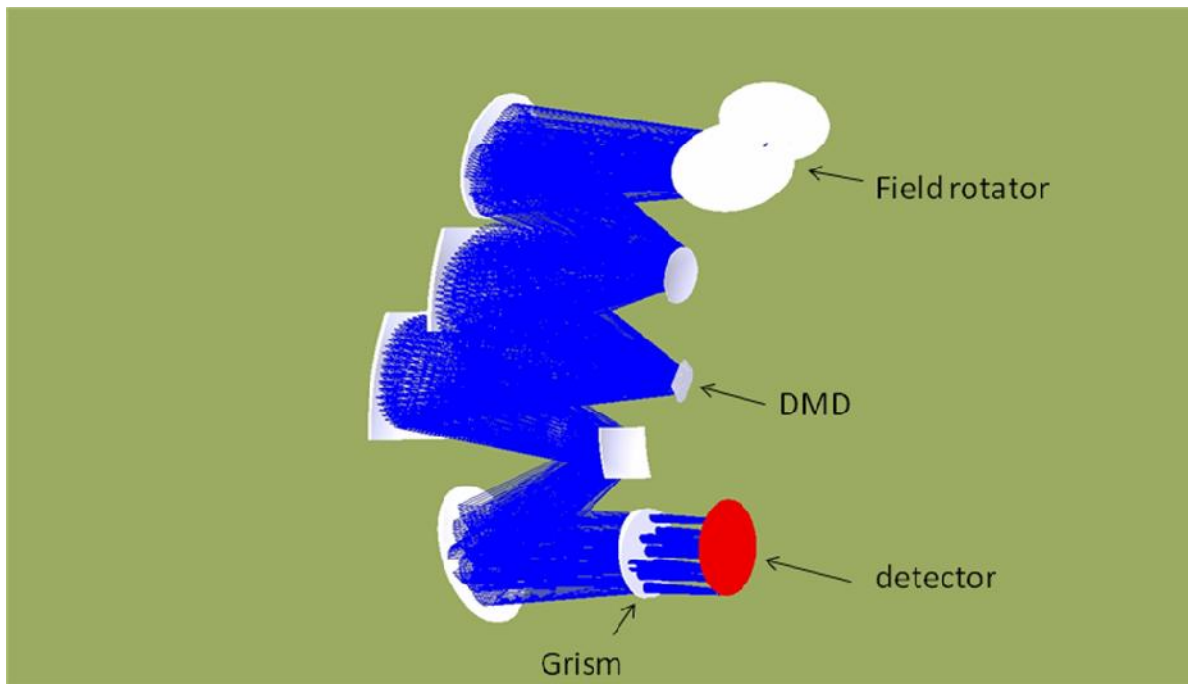


Fig. 5. View of one NIR spectrograph channel of the grism-and-mirror option.

6. GRISM-AND-MIRROR SPECTROGRAPH DESIGN

6.1 Design Guidelines

The Euclid multislit spectrograph is based on a commercial Texas Instrument device known as Cinema DMD which is able to move independently 2.2 millions (2K x 1.05K) micromirrors. The basic idea is to keep unchanged the Visible and NIR imagery channels of the Euclid mission and simply add the NIR spectrograph channels while maximizing the field of view (FOV) per DMD with the goal to reach the same value than the imagery channel (0.5 deg^2) by using a few spectrographs. Among different possibilities it rapidly appeared that picking off several subfields at the intermediate Cassegrain focus of the TMA telescope was an attractive solution in terms packaging and independence between the imaging and spectroscopic channels. The price to pay is to deal with a strongly aberrated and curved intermediate focal plane.

Each DMD square mirror (13.7 micrometers) can rotate by ± 12 degrees around its diagonal. This tilt angle gives an upper limit on the F-number of the beam coming and exiting the DMD device. To keep a small margin we choose to have a $F/2.7$ beam striking the DMD at an angle of 24 deg . In this configuration the reflected beam is normal to the DMD surface. Some spectra are truncated however. Once the speed of the beam is chosen, the maximum FOV seen by each DMD is frozen. With the above assumptions the corresponding FOV on the sky is $0.44 \times 0.24 \text{ deg}^2$ (0.105 deg^2) per DMD.

The first optical challenge is to produce a fast converging beam onto the DMD with a 24° angle and an excellent image quality (less than the DMD mirror size of $13.7 \mu\text{m}$) over a flat field. The second optical challenge is to design a spectro-imager fed by the fast beam reflected by the DMD. The spectro-imager must have a magnification of ~ 2.6 in order to have a DMD mirror ($13.7 \mu\text{m}$) corresponding to two pixels ($2 \times 18 \mu\text{m} = 36 \mu\text{m}$) on the NIR detector. Giving this sampling, two 2Kx2K NIR detectors are needed to cover the image from a single Cinema DMD.

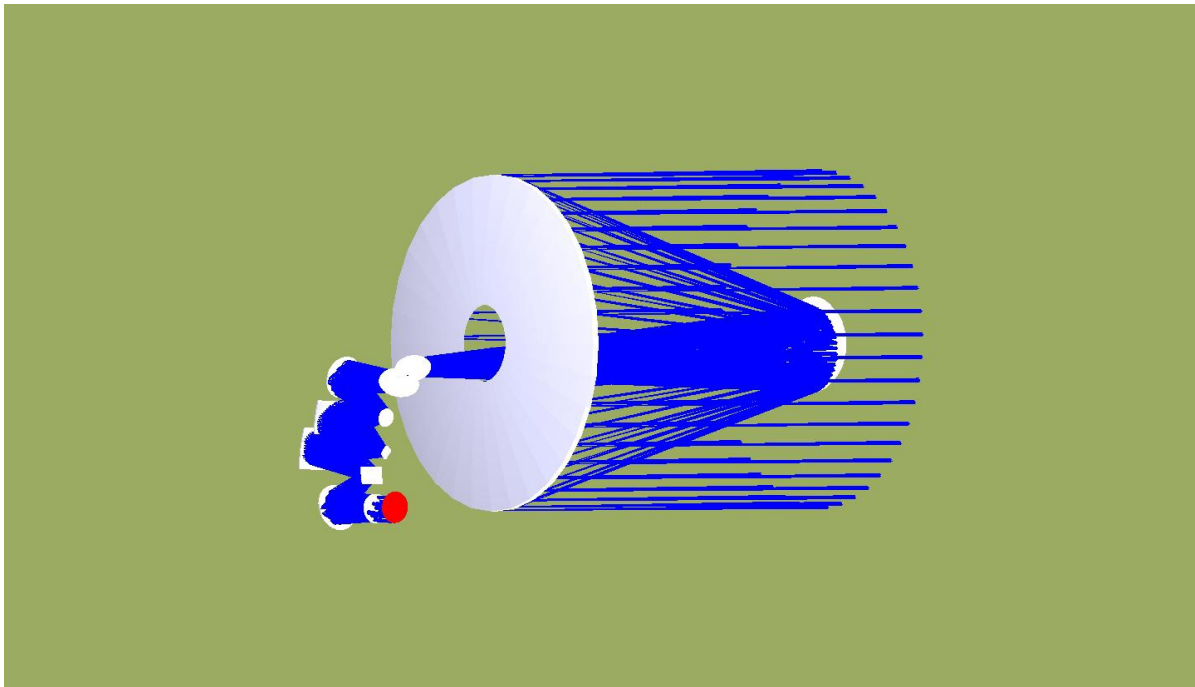


Fig. 6. One grism-and-mirror NIR spectro-imaging channel behind the Euclid telescope.

6.2 Design Overview

The concept includes a field rotator composed of two flat mirrors with the ability to pick off the beam and redirect it in an orientation that optimizes the packaging of the whole spectrograph channels. The second element is the fore-optics acting as a focal reducer that feeds each DMD with the required angle and speed. The third element is an imaging spectrograph capable of spectroscopy by the insertion of a grism, or imagery by inserting a lens and a filter. This concept therefore enables both NIR spectroscopy and NIR imaging.

6.3 Fore-optics

The fore-optics is composed of eccentric and tilted portions of aspheric surfaces (fig. 5). Presently the corresponding FOV on the sky is $0.44 \times 0.24 \text{ deg}^2$ or 0.105 deg^2 with a parallelogram shape since some anamorphism is present in the design. Some spectra are also truncated. With the present design 80% of encircled energy is within a 12 microns diameter for 9 points in the field covering the entire DMD.

Table 2. Overall performance of grism-and-mirror spectrograph.

Parameter	Value
Observing modes	<ul style="list-style-type: none">• Broadband Imaging• Multi-slit spectroscopy
Field of View	$0.44 \times 0.48 \text{ deg}^2$ (0.21 deg^2) for two channels
Wavelength range	1 – 1.7 μm
Spectral Resolution	<ul style="list-style-type: none">• 280 @ 1 μm• 375 @ 1.35 μm• 470 @ 1.7 μm
Slit sampler	2 'CINEMA' DMDs, 2K \times 1.05K, 13.7 μm mirrors
Detectors	4 2K \times 2K NIR arrays, 18 μm pixels
Optical train	2 folding mirror, 3 mirrors, 1 DMD, 3 mirrors, 1 disperser, filter(s)
Spectral sampling	Slit with one DMD micro mirror is sampled by ~ 2 detector pixels

6.4 Grism-and-mirror spectro-imager

The grism-and-mirror spectro-imager is composed of three aspheric surfaces (fig. 5), and gives a magnification of 2.6 to get ~ 2 pixels on the image of a single micro-mirror. The dispersive element of the spectroscopic mode is a grism located in the final convergent beam. This configuration yields a simpler and more compact design than the more classical configuration where the disperser is placed in a collimated beam between a collimator and a camera.

The 100 mm diameter grism is made of a 3.6° fused silica prism with a groove density of 70 g/mm. This grism is located 140 mm before a pair of 2K \times 2K detectors. With the present design 80% of encircled energy is within a 36 microns diameter for all points in the field and for the whole bandwidth. Given the grism characteristics and the 1-1.7 μm bandwidth, the length of a spectrum is 7 mm. The number of spectral elements (taken as 2 detector pixels) is then 194 which yields a resolving power of $R = 374$ at 1.35 μm .

6.5 Overall System

Given the compactness of the proposed design (700 mm x 600 mm) and the use of field rotators, three spectrographs can easily be implemented together with the visible/NIR imaging channel. All the spectrographs could be installed on a unique bench parallel to the 1.2 meters primary mirror of Euclid since the height is less than 200 mm (fig. 6).

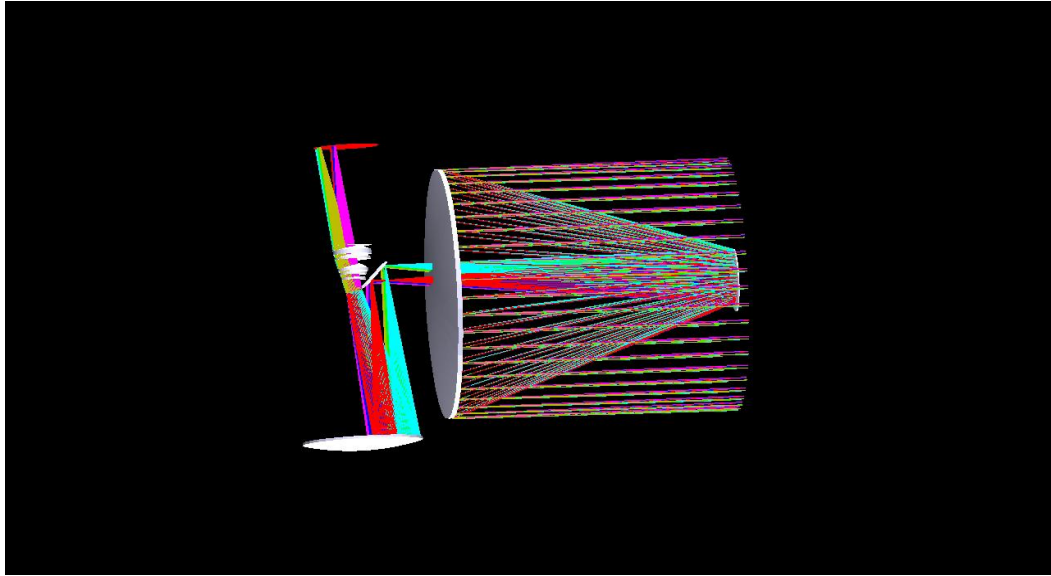


Fig. 7. General view of the backup slitless channel with the Euclid telescope

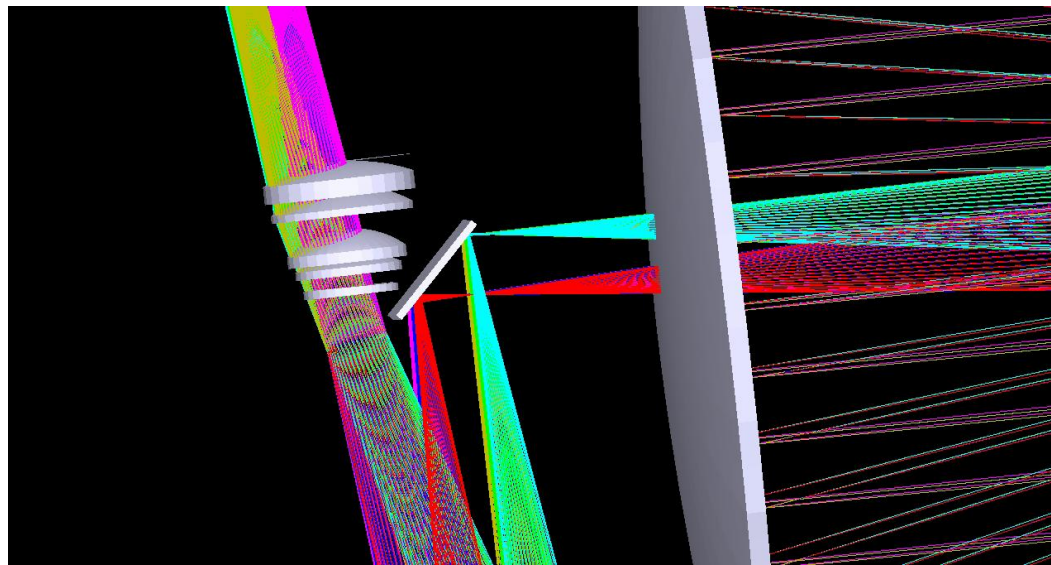


Fig. 8. Closer view showing the grism and the four lenses

7. SLITLESS CHANNEL AS A BACKUP SOLUTION IN CASE OF DESCOPE OF THE DMDS

A rectangular subfield of $0.5^\circ \times 1^\circ$ is picked off at the intermediate Cassegrain focus and redirected to a dedicated tertiary mirror to form an 80 mm pupil where a grism is located. With the assumption of having 8 NIR detectors only allocated to this slitless channel, the focal of the telescope has to be reduced to match the required FOV. We adopted a dioptric design where four lenses transform the initial F/20 beam exiting the tertiary to an F/7 beam (fig. 7 & 8). With the present design remains a slight curvature of the focal surface. The grism has a low groove density (17 l/mm) and the

prism angle of its silica substrate is 1° . The bandwidth extends from 1 to $1.7 \mu\text{m}$ with a spectrum length of 6.4 mm giving a spectral resolution ranging from $R = 253 @ 1 \mu\text{m}$ up to $R = 431 @ 1.7 \mu\text{m}$.

8. LARGE FIELD PRISM-AND-MIRROR SPECTROGRAPH DESIGN

This design is similar to the original design in the SPACE proposal but with significantly less optics ^[3]. A complete description is available in reference ^[4] in these proceedings. The telescope is a Korsch 3 mirror design similar to the original design of DUNE ^[5] but with some modifications to make space for the EUCLID spectrograph channel. A system of 3 pick-off mirrors is placed on the intermediate focal plane between the secondary and tertiary of the telescope. They cut the field in 3 parts. Each is re-imaged on a DMD by a system of 3 mirrors that we call the DMD fore-optics. These optics also fasten the beam to get a large field of view on the small DMD. A difficulty comes from the large incident angle on the DMD which is 27° from the vertical. The beam need to be faster in the plane perpendicular to the DMD that contains the incident chief ray in order to get the same magnification in both directions. Otherwise, the field would be stretched by a factor of $1/\cos(27^\circ)$ in one direction. The beam is then $F/2.2 \times F/2.5$ which gives a micromirror size of 0.94". This fast beam and high incident angle was necessary to get a sufficiently large field of view of $0.82^\circ \times 0.57^\circ$. Special care has been taken to get a design giving little distortion on the DMD so that the original rectangular field fit well on the DMD then avoiding losses.

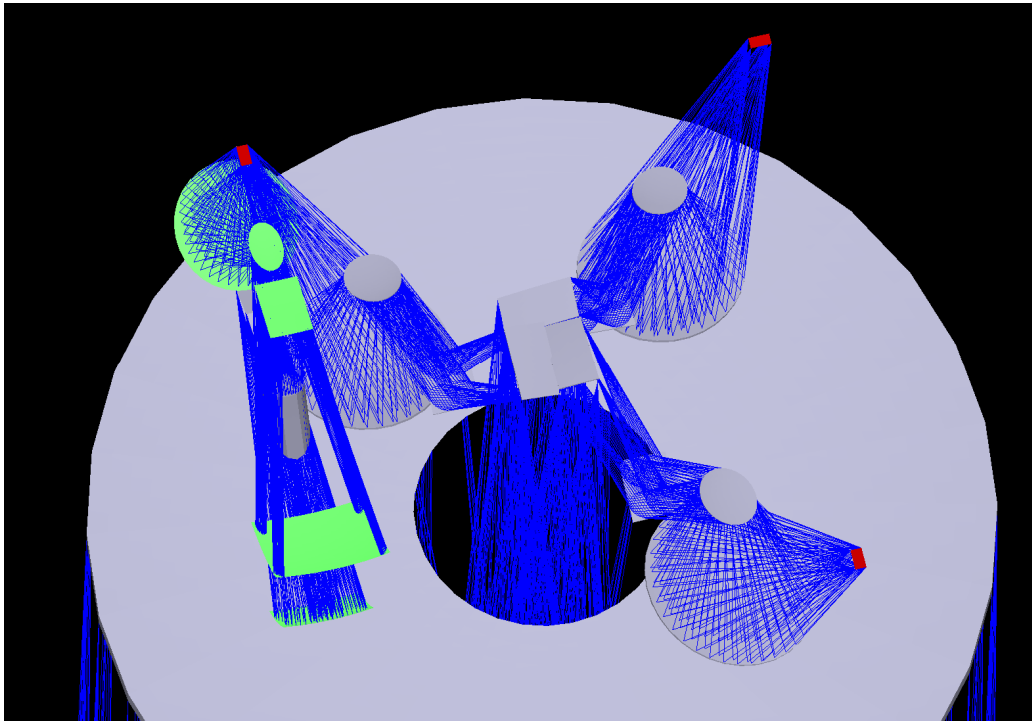


Fig. 9. View of the large field prism-and-mirror EUCLID spectrograph channel with only one of 3 spectrographs shown. The red rectangles are the DMDs.

A spectrograph follows each DMD. The collimator is made of 4 mirrors; this relatively large number is necessary to get the pupil on the prism disperser considering the fast beam and the needed image quality. The glass of the prism has been carefully chosen to make the spectral resolution as a function of wavelength as constant as possible. This is one of the many advantages of a prism compared to a grating type of dispersor; the slope of the spectral resolution as a function of wavelength can be adjusted to maximize the scientific return by choosing the correct glass. After the prism, the camera is made of only one mirror. In the original SPACE design, the camera was made of 4 lenses and 2 fold mirrors. Collimator

and camera had been designed separately for SPACE and the beam was perfectly collimated on the prism. This was not possible with the new design. Collimator and camera must work together to obtain the correct image quality on the detector. The beam is then not telecentric on the prism.

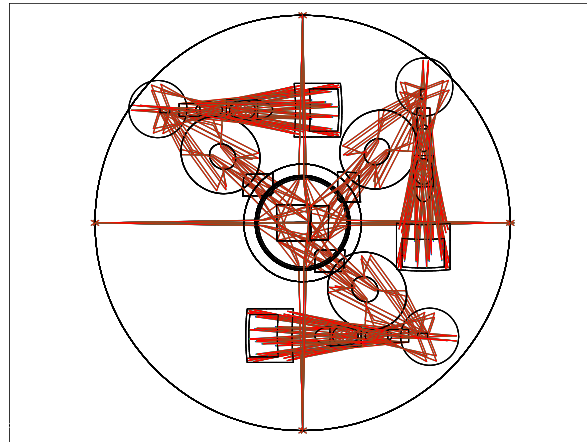


Fig. 10. Top view of the EUCLID spectrograph channel with all spectrographs shown.

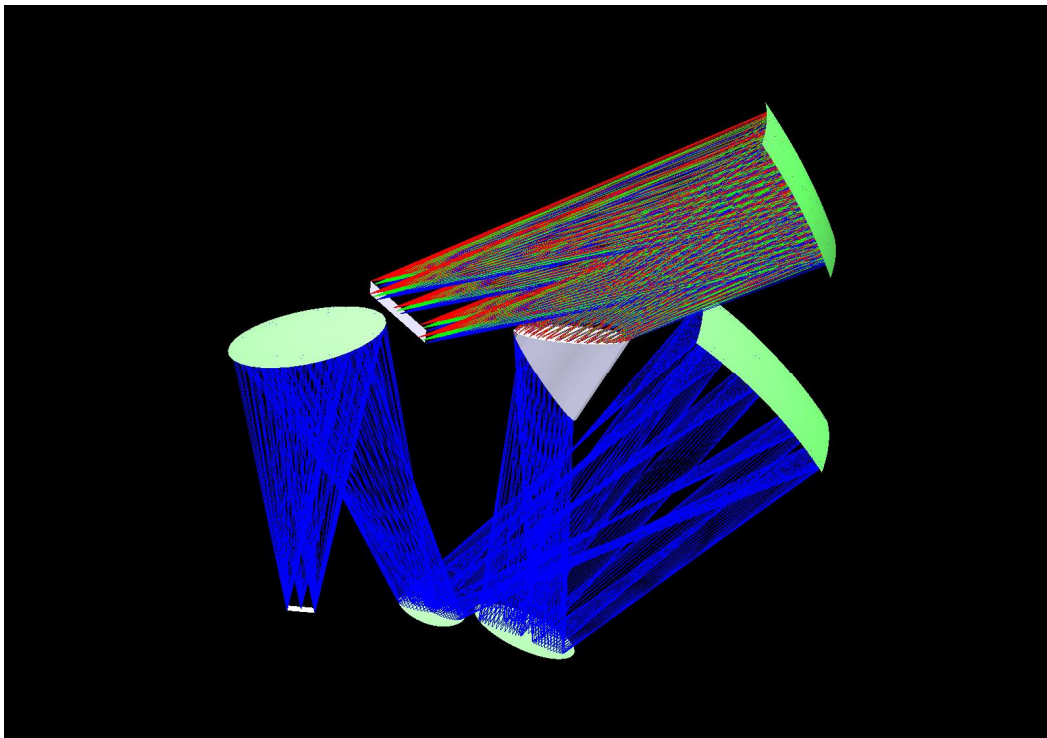


Fig. 11. View of one of the 3 EUCLID prism-and-mirror spectrographs.

This non-collimated design generated a difficulty for adding an imaging capability to the spectrograph. While there is an independent NIR photometric channel in the DUNE part of the mission, an imaging capability is still requested for the spectrographs. If the beam was perfectly collimated at the prism, a fold mirror replacing the prism would be sufficient to get an image on the detector. This was in the original design of SPACE. With the EUCLID spectrograph channel, a

simple mirror would give a very bad image quality because the camera corrects the aberration of the collimator and prism; with the fold mirror, the rays do not hit the camera mirror at the correct position. The solution was to design a grism very similar in size to the prism. In this design, the grating function in reverse; it cancels the dispersion of its associated prism.

This design was used by ESA to make a mechanical design (fig. 12) which showed that this optical design respects the limits of space envelope and weight.

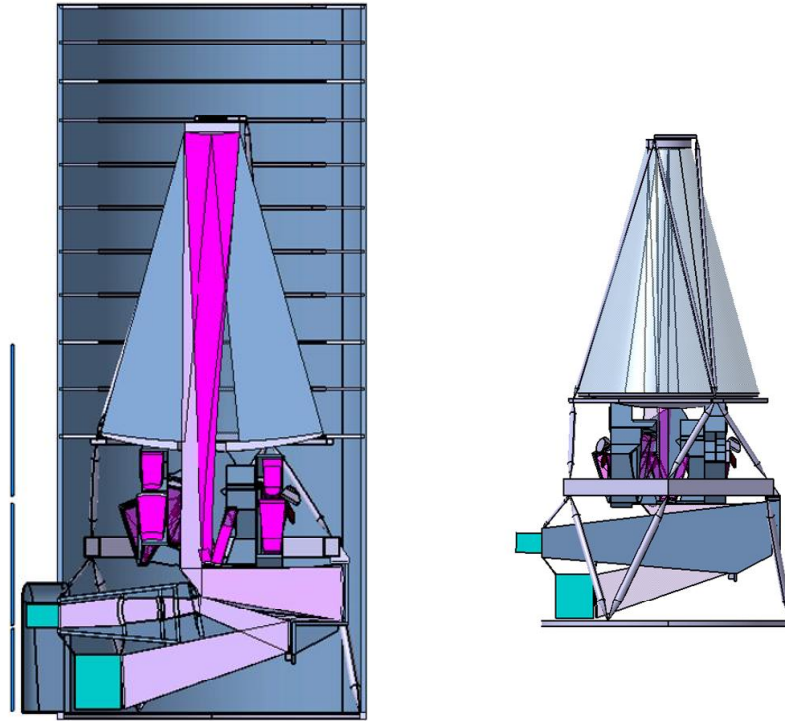


Fig. 12. ESA mechanical design based on the prism spectrograph optical design; a specific design of the visible and NIR photometric channels (ex-DUNE), had to be made to fit with the spectrograph design.

9. CONCLUSION

Our work showed that many solutions worth studying for the design of the EUCLID spectrograph channel. All give good image quality. The ESA mechanical design of the prism spectrograph channel and its associated visible and NIR photometric channel further prove that the design respect the limits of weight and volume. All aspects of the mission have been studied and no show stoppers have been found so far.

REFERENCES

- [1] Riess, A.G., et al., "Observational Evidence from Supernovae for an Accelerating Universe and a Cosmological Constant", *AJ* 116, 1009 (1998).
- [2] Perlmutter, S., et al., "Measurements of Omega and Lambda from 42 High-Redshift Supernovae", *ApJ* 517, 565 (1999).
- [3] Cimatti, A., et al., "SPACE: the SPectroscopic All-sky Cosmic Explorer", arXiv0804.4433, - (2008).
- [4] Content, R., "Durham Optical Design of EUCLID, the Merged SPACE/DUNE ESA Dark Energy Mission", *Proc. SPIE 7010, These Proceedings* (2008).
- [5] Refregier, A., "The Dark Universe Explorer (DUNE): proposition to ESA's cosmic vision", *Proc. SPIE 7010, These Proceedings* (2008).